Long-Range Repulsive Interaction between Molecules on a Metal Surface Induced by Charge Transfer

I. Fernandez-Torrente,[1] S. Monturet,[2] K. J. Franke,[1] J. Fraxedas,[3] N. Lorente,[2,3] and J. I. Pascual[1]

[1]*Institut für Experimentalphysik, Freie Universität Berlin, Arnimallee 14, 14195 Berlin, Germany*
[2]*Laboratoire Collisions, Agrégats, Réactivité, UMR5589, Université Paul Sabatier,
118 route de Narbonne, 31062 Toulouse cédex, France*
[3]*Centre d'Investigació en Nanociència i Nanotecnologia (CIN2-CSIC-ICN), Edifici CM-7,
Campus de la UAB, E-08193 Bellaterra, Spain*
(Received 24 June 2007; published 25 October 2007)

The adsorption of a molecular electron donor on Au(111) is characterized by the spontaneous formation of a superlattice of monomers spaced several nanometers apart. The coverage-dependent molecular pair distributions obtained from scanning tunneling microscopy data reveal an intermolecular long-range repulsive potential, which decreases as the inverse of the molecular separation. Density functional theory calculations show a charge accumulation in the molecules due to electron donation into the metal. Our results suggest that electrostatic repulsion between molecules persists on the surface of a metal.

The spontaneous formation of self-organized molecular structures at metal surfaces follows a complex balance of interactions between the basic functional units [1]. Attractive short-range forces between molecules are ubiquitous during growth, but their strength and relevance varies depending on the molecular functionalization. For the case of adsorption on metal surfaces, these forces compete with substrate-mediated interactions, for example, through elastic stress fields [2–4] or through surface-state electrons [5–12]. These usually extend for larger length scales than intermolecular dispersion forces and can lead to characteristic nearly periodic arrays of particles [10,11]. Long-range interactions can also have a repulsive nature. This is the case of electrostatic interactions between charged particles weakly interacting with a nonconducting host support [13,14] or in ensembles of organic molecules with large dipolar moments on metal surfaces [15,16].

Apolar and neutral molecules are not expected to build up long-range interaction potentials other than those mediated by the underlying substrate [9], and, in most cases, attractive dispersion forces lead to nucleation in two- or three-dimensional condensates. Charge redistribution upon molecular chemisorption is also capable of rendering interesting changes in the interaction potentials between molecules [17]. Although this effect is presumably strong in charge transfer adsorbate systems, it has been usually neglected due to the screening nature of metallic substrates. An experimental proof of its relevance in intermolecular interactions is thus still missing. This could also help to build up a quantitative picture about fundamental processes related to molecular charging on metal surfaces.

Here we report on the spontaneous formation of nearly periodic superlattices of single tetrathiafulvalene (TTF: $C_6H_4S_4$) molecules on an Au(111) surface. TTF is well known as a prototype donor molecule in charge transfer compounds [18]. The free molecule has no electrical dipole moment. However, on Au(111), it becomes charged upon electron donation. Using a combination of low-temperature scanning tunneling microscopy (STM) and density functional theory (DFT), we resolve that a repulsive long-range interaction between charged molecules is built up, thus hindering nucleation of islands. The coverage-dependent intermolecular potential wells forming the molecular superlattice, reconstructed through the analysis of molecular pair distributions, are consistent with a long-range interaction driven by the electrostatic repulsion between molecules. This suggests that local charges at the interface induced upon chemisorption cannot be quickly screened in the surface of metallic substrates.

In our experiment, an atomically clean Au(111) substrate is exposed to a flux of TTF molecules sublimated from a homemade Knudsen cell under ultrahigh vacuum. Posteriorly, the sample is inserted in our custom-made low-temperature STM, where measurements are performed at a temperature of 5 K. Depositing a small amount of TTF (<0.1 ML) on the metal at room temperature leads to the formation of a characteristic one-dimensional array of TTF monomers along the fcc regions of the Au(111) $23 \times \sqrt{3}$ reconstruction [Fig. 1(a)]. The monomers' pair distances are homogeneous for a given coverage, with an average value amounting to several nanometers [~3 nm for the data in Fig. 1(a)]. This distance is significantly larger than the typical length scale of attractive noncovalent interactions.

The formation of the superlattice of TTF monomers needs to be thermally activated. When TTF is dosed on a 80 K cold sample [Fig. 1(b)], monomers and small TTF clusters appear randomly spread and are easily dragged by the STM tip (probably they populate a weakly adsorbed precursor state). Only upon annealing, do the molecules self-organize, forming the distinctive nearly periodic array
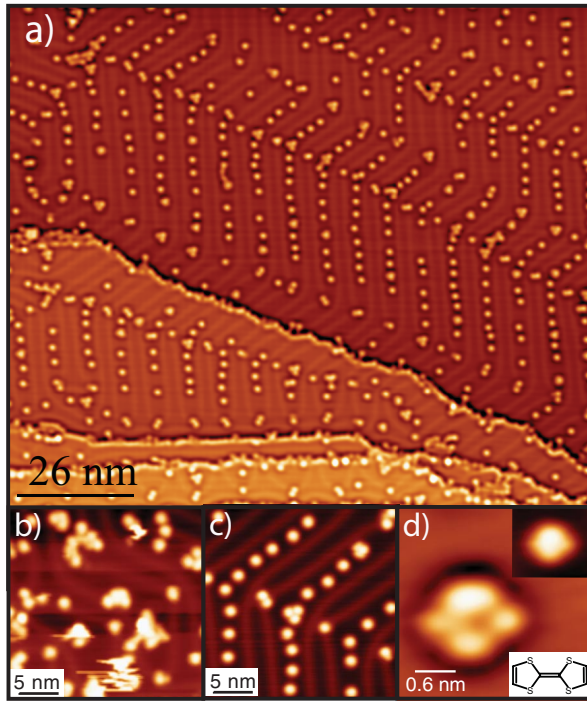
FIG. 1 (color online). (a) STM image of an Au(111) region with 0.03 ML of TTF deposited at room temperature. (b) TTF molecules deposited on a cold sample (80 K). (c) After annealing to room temperature, the TTF arrays along fcc regions are formed. (d) STM image (inset; $Vs = -1$ V) and its Laplace filtered image [30] of a TTF molecule. The latter reveals that two of the sulfur atoms appear brighter, suggesting a small tilt of the molecular plane with respect to the surface.

FIG. 2 (color online). (a)–(c) STM images of TTF on Au(111) at various coverages. (d) Pair distributions f of the one-dimensional TTF arrays for the data shown in Fig. 1 (0.03 ML) and (a)–(c). For 0.08 and 0.16 ML, the distributions are performed on hcp regions. More than 500 pairs are analyzed in each plot. The molecular coverage is determined from STM images of large surface areas, assuming that 1 ML corresponds to 2 molecules/nm^2. From the lowest to the largest coverage, we obtain an *average* pair distance $\bar{r}$ of 3.5, 2.5, 3.3, and 1.7 nm in the one-dimensional arrays. The corresponding 1D distribution functions for noninteracting particles f_{ran} are included.

[Fig. 1(c)]. In this case, high-resolution STM images [Fig. 1(d)] of the intramolecular structure can be obtained. At negative sample bias, TTF appears with a characteristic asymmetry in the images, resembling two of the lateral S atoms being higher than the other two.

The results of Fig. 1(a) show that (for low-coverage and after annealing) TTF does not respond to attractive forces such as, for example, hydrogen bonding to sulfur atoms [19]. This also prevails as the coverage is increased, accompanied by a monotonous decrease in the average pair distance [Figs. 2(a)–2(c)]. At 0.08 monolayers (ML), the array is compressed (average pair distance ~2 nm) into double rows of monomers in the fcc regions of the reconstruction. Close to this coverage, hcp regions start also to be populated with similar one-dimensional arrays of TTF monomers. The tendency to avoid nucleation through the formation of nearly periodic molecular arrays is indicative of a long-range interaction mechanism different from (shorter-range) noncovalent dispersion forces between molecules.

Elastic deformation of the substrate can lead to long-range interactions between adsorbates [2,3,5]. The induced stress field can oppose the approach of two adsorbates becoming the driving force of an ordered phase. Indeed, the Au(111) herringbone reconstruction is itself a stressed

atomic layer, folded with a periodicity very sensitive to changes of the elastic energy. We find that the herringbone structure is unaffected by submonolayer TTF coverages. Hence, this mechanism is improbable in our case. An alternative long-range interaction between atoms [8,10] or molecules [9] on metal surfaces is the oscillatory potential associated with the Friedel oscillations of surface-state electrons. A key element here is the oscillatory character of the interaction with a period related to half of the Fermi wavelength ($\lambda_F/2$). However, the average pair distance ($\bar{r}$) in Fig. 2 is larger than $\lambda_F/2$ for Au(111) (1.8 nm) and decreases monotonously with TTF density along the rows. Thus, an interaction mediated by surface electrons can also be discarded as the driving force leading to the superlattice formation.

Figure 2(d) shows the pair distance r distributions of one-dimensional arrays for various coverages (along fcc regions or hcp regions, depending on the coverage). For a one-dimensional system of noninteracting particles, the first-neighbors random pair distribution function f_{ran} decays monotonically with the pair distance r as shown by a dashed line in Fig. 2(d). The peaked distributions in Fig. 2(d) are symptomatic of a repulsive long-range interaction between monomers. Motivated by the donor nature of TTF as a free molecule, we have performed *ab initio* calculations in order to trace back the nature of the

molecule-surface interaction and its effect in the long-range repulsion between TTF monomers.

We have used DFT within the generalized gradient approximation [22] as implemented in the VASP code [23] to evaluate the properties of a relaxed layer of TTF on an artificial fcc (111) four-layer slab of gold atoms. The electron-ion interaction is described by the projector-augmented wave scheme [24]. A large unit cell (6×4) is employed in order to account for large molecular separations within computationally reasonable limits.

The relaxed TTF structure [Fig. 3(a)] reveals that the molecule-surface interaction is driven by local S–Au bonds. Because of the incommensurate dimensions of molecule and surface, the local interactions lead to an asymmetric chemisorption of the molecule. As a result, the molecule aligns along the $\{1\bar{1}0\}$ direction of the surface
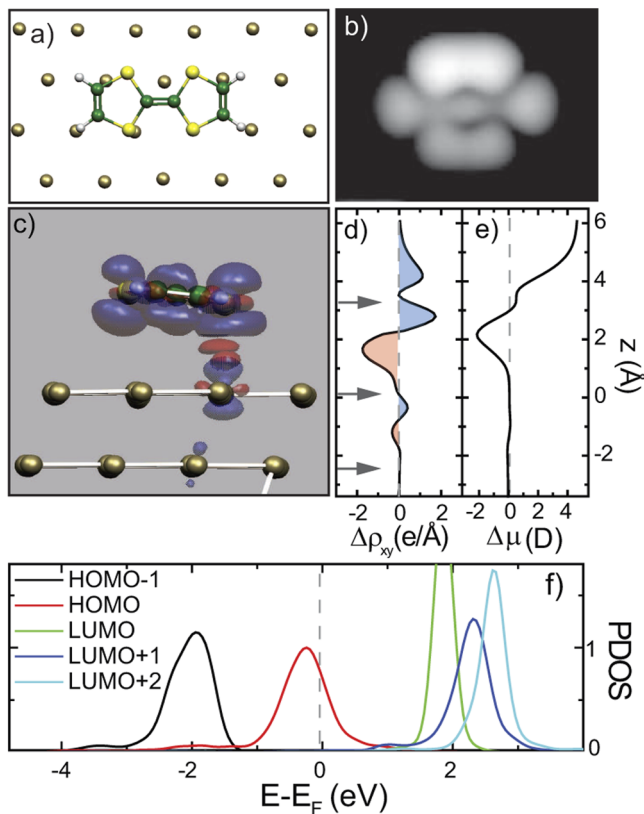
FIG. 3 (color online).   Results from DFT simulations. (a) Fully relaxed configuration of TTF on Au(111). The uppermost two gold layers as well as the molecular degrees of freedom are relaxed until atomic forces are lower than 0.01 eV/Å. (b) Tersoff-Hamman constant current image [25] of the molecule in (a) ($V = -0.5$ V). (c) Induced electronic density by the molecule-surface interaction. (d) Lateral (x-y planes) integration of the induced charge. The arrows show the vertical distance values at which the two topmost surface layers and the two binding S atoms lie. (e) Accumulated induced dipole. Together with (d), it reveals that the molecule becomes positively charged. (f) Projected density of states on molecular orbitals. The electronic states with HOMO character are partially empty, in agreement with the data of (c)–(e).

and tilts 8° with respect to the surface plane. The tilt is responsible for the asymmetry in the experimental constant current STM image [Fig. 1(d)], as it is here captured by its Tersoff-Hamman simulation [25] [Fig. 3(b)]. At negative bias voltage, the STM image is basically dominated by the shape of the highest occupied molecular orbital (HOMO).

The local interaction character between Au and S atoms implies a sizable bonding strength and a large charge donation into the surface. Indeed, the adsorption energy after dipole corrections is -0.86 eV, and the surface-molecule distance is 2.76 Å. The electronic structure of the S atoms has a large contribution in the HOMO, which causes a large redistribution of electronic charge [Fig. 3(c)]. The charge donation is expressed by a partial decrease of the electron density in the whole molecular plane. The result is a positive charging of the molecule and the creation of a surplus of negative charge localized close to the S–Au bonds. Figure 3(d) shows the planar integration of charge. An excess of positive charge ($\sim 0.6e$) is located around the molecule, and the corresponding screening negative charge ($\sim -0.4e$) is between the molecule and the first atomic layer. The molecule-surface interaction leads to a large surface dipole that is evaluated in Fig. 3(e) according to Ref. [26]. The dipole is zero inside the surface and builds up across the molecule reaching a value of 5.0 D.

The charge donation gleaned from the induced electronic density causes the partial emptying of the HOMO. This is clearly seen by plotting the projection of the full electronic structure onto the molecular orbitals corresponding to the present molecular conformation [Fig. 3(f)] [27]. The molecule-surface interaction also broadens the molecular features associated to the HOMO-1, HOMO, and the lowest unoccupied molecular orbital (LUMO), revealing a substantial hybridization with the surface electronic structure, while higher-lying resonances are thinner, showing their small role in the molecular-surface interaction.

The *ab initio* results evidence a significative charging of the TTF on the Au(111) surface. To clarify its role in the formation of the arrays, we analyze the statistics shown in Fig. 2(d). The experimental pair distribution f arises from the site occupation as dictated by the Boltzmann factor $\exp\{-[\omega(r) - \mu]/k_B T\}$, where $\omega(r)$ is the *mean* interaction potential behind the formation of the superlattice, μ is a (coverage-dependent) zeroth order potential [28], and k_B is the Boltzmann constant. To evaluate $\omega(r)$, we divide the experimental pair distribution f by that of noninteracting particles (f_{ran}) and plot $-\ln(f/f_{\mathrm{ran}})$ (Fig. 4). In the limit of a very dilute system [8,10,21], i.e., where no superlattice is formed, $\omega(r)$ would be a good approximation to the (repulsive) pair interaction potential $E(r)$. Here, however, $\omega(r)$ has the shape of a potential well. As the molecular density increases, the well becomes more symmetric and shallower, in accord with the TTF molecules being confined into sharper pair distributions and, hence, forming a superlattice. Unfortunately, it is not trivial to obtain the
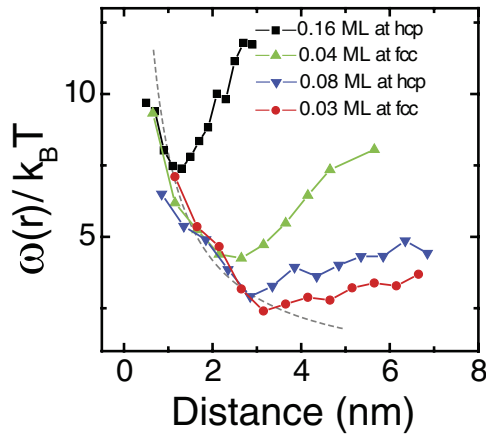
FIG. 4 (color online).   Mean interaction potentials $\omega(r)$ of one-dimensional TTF arrays obtained from the pair distributions shown in Fig. 2(d). The dashed line represents the pair electrostatic interaction $E(r)$ between particles charged with $0.3e$ and a temperature ($T = 160$ K) to fit the repulsive part of $\omega(r)$ for the most dilute case. Each curve has been shifted upwards an amount (8.4, 5.4, 4.1, 3.8, from top to bottom) representing the coverage-dependent zeroth order internal potential and approximated here as the electrostatic energy per molecule in a fully periodic lattice and using the fitted temperature, for consistency. Note that the range of the interaction energy obtained from this fitting (30–100 meV) is considerably larger than the energy of a long-range interaction mediated by surface electrons [8].

shape of the pair interaction $E(r)$ from the mean potential $\omega(r)$ [29]. However, we note that for small pair distances $\omega(r)$ decays as $1/r$ and is consistent with an electrostatic repulsion between molecules charged with $0.3e$, as is described in the *ab initio* results.

The interaction mechanism suggested from Fig. 4 entails that the metal bulk electrons cannot completely screen the local charge on the surface. At the position of the molecule, a large part of the metal density of states comes from the Shockley surface state, whose Fermi wavelength amounts to 3.6 nm. Hence, we presume that the electrostatic field created by the molecular charge can extend for a few nanometers due to the larger screening length of surface states.

In summary, our study reveals a repulsive interaction between charged molecules on a metal surface that leads to the formation of a molecular array resembling a (one-dimensional) Wigner crystal. Its origin is here attributed to the Coulomb repulsion among localized charges built up at the molecule-surface interface by charge redistribution occurring upon chemisorption. A direct consequence is that the screening length of a charge on a metal surface extends for several nanometers, probably due to the role of surface states. We expect that such long-range repulsion can be a fingerprint of charge transfer processes at organic molecule–metal interfaces.

[1] G. M. Whitesides and R. F. Ismagilov, Science **284**, 89 (1999).
[2] H. Brune *et al.*, Nature (London) **394**, 451 (1998).
[3] K. Pohl *et al.*, Nature (London) **397**, 238 (1999).
[4] K. H. Lau and W. Kohn, Surf. Sci. **65**, 607 (1977).
[5] K. H. Lau and W. Kohn, Surf. Sci. **75**, 69 (1978).
[6] D. J. Keller, H. M. McConnell, and V. T. Moy, J. Phys. Chem. **90**, 2311 (1986).
[7] P. Hyldgaard and M. Persson, J. Phys. Condens. Matter **12**, L13 (2000).
[8] J. Repp *et al.* Phys. Rev. Lett. **85**, 2981 (2000).
[9] S. Lukas, G. Witte, and Ch. Wöll, Phys. Rev. Lett. **88**, 028301 (2001).
[10] N. Knorr *et al.*, Phys. Rev. B **65**, 115420 (2002).
[11] F. Silly *et al.*, Phys. Rev. Lett. **92**, 016101 (2004); M. Ternes *et al.*, Phys. Rev. Lett. **93**, 146805 (2004).
[12] S. U. Nanayakkara *et al.*, Phys. Rev. Lett. **98**, 206108 (2007).
[13] K. Wierschem, Int. J. Mod. Phys. B **20**, 2667 (2006).
[14] M. Sterrer *et al.*, Phys. Rev. Lett. **98**, 096107 (2007).
[15] T. Yokoyama *et al.*, Phys. Rev. Lett. **98**, 206102 (2007).
[16] A. E. Baber *et al.*, J. Am. Chem. Soc. **129**, 6368 (2007).
[17] E. C. H. Sykes *et al.*, J. Am. Chem. Soc. **127**, 7255 (2005).
[18] J. Fraxedas, *Molecular Organic Materials: From Molecules to Crystalline Solids* (Cambridge University Press, Cambridge, England, 2006).
[19] F. Wennmohs, V. Staemler, and M. Schindler, J. Chem. Phys. **119**, 3208 (2003).
[20] f_{ran} can be exactly obtained from a combinatorial analysis as $f_{\mathrm{ran}} = n!(N - r_s)!(N - n)!/[(N!(N - r_s - n + 1)!]$, where n is the number of particles in a box with N sites and r_s is the pair distance r in units of sites. Note that f_{ran} decreases monotonically with r_s in a one-dimensional ensemble [8,10,21].
[21] T. T. Song, Phys. Rev. Lett. **31**, 1207 (1973).
[22] J. P. Perdew *et al.*, Phys. Rev. B **46**, 6671 (1992).
[23] G. Kresse and J. Fürthmuller, Comput. Mater. Sci. **6**, 15 (1996).
[24] G. Kresse and D. Joubert, Phys. Rev. B **59**, 1758 (1999).
[25] J. Tersoff and D. R. Hamman, Phys. Rev. Lett. **50**, 1998 (1983).
[26] L.-L. Wang and H. P. Cheng, Phys. Rev. B **69**, 165417 (2004).
[27] N. Lorente *et al.*, Phys. Rev. B **68**, 155401 (2003).
[28] μ represents the internal energy per molecule of a dense system of interacting particles, being the chemical potential in the limit of infinite number of particles.
[29] B. Diu *et al.*, *Physique Statistique* (Hermann, Collection enseignement des sciences, Paris, 1997).
[30] I. Horcas *et al.*, Rev. Sci. Instrum. **78**, 013705 (2007).